

Production of the pentaquark Θ^+ in np scattering

Seung-II Nam,^{1,2,*} Atsushi Hosaka,^{1,†} and Hyun-Chul Kim^{2,‡}

¹Research Center for Nuclear Physics (RCNP), Ibaraki, Osaka 567-0047, Japan

²Department of Physics and Nuclear Physics & Radiation Technology Institute (NuRI), Pusan National University, Busan 609-735, Korea

(Received 1 March 2004; published 16 December 2004)

We study $np \rightarrow \Lambda\Theta^+$ and $np \rightarrow \Sigma^0\Theta^+$ processes for both of the positive and negative parities of the Θ^+ . Employing the effective chiral Lagrangians for the KNY and K^*NY interactions, we calculate differential cross sections as well as total cross sections for the $np \rightarrow \Sigma^0\Theta^+$ and $np \rightarrow \Lambda\Theta^+$ reactions. The total cross sections for the positive parity Θ^+ turn out to be approximately 10 times larger than those for the negative parity Θ^+ in the range of the c.m. energy $E_{\text{c.m.}}^{\text{th}} \leq E_{\text{c.m.}} \leq 3.5$ GeV. The results are rather sensitive to the parameters of K exchanges in the t channel.

DOI: 10.1103/PhysRevD.70.114027

PACS numbers: 13.75.-n, 12.39.Mk, 13.75.Cs

I INTRODUCTION

Since the experimental finding of the lightest *pentaquark* baryon Θ^+ [1] motivated by the work of Ref. [2], the physics of the pentaquark states has been a hot issue. The DIANA [3], CLAS [4], SAPHIR [5], HERMES [6], and SVD [7] Collaborations and the reanalysis of neutrino data [8] have confirmed its existence. The Θ^+ has unique features: It has a relatively small mass and a very narrow width. The exotic Ξ states found recently by the NA49 Collaboration [9] share the features similar to the Θ^+ . While a great amount of theoretical effort has been put into understanding properties of the Θ^+ [10–16], there is no consensus in determining the parity of the Θ^+ . For example, chiral models predict the parity of the Θ^+ to be positive [11], whereas the lattice QCD and the QCD sum rule prefer the negative parity [14,15].

Many works have suggested different ways of determining the parity of the Θ^+ [17–25], among which Thomas *et al.* [18] have proposed an unambiguous method to determine the parity of the Θ^+ via polarized proton-proton scattering at and just above the threshold of the Θ^+ and Σ^+ : If the parity of the Θ^+ is positive, the reaction is allowed at the threshold region only when the total spin of the two protons is $S = 0$; if negative the reaction is allowed only when $S = 1$. Hence it is very challenging to measure such a process experimentally [26]. Triggered by Thomas *et al.* [18], Hanhart *et al.* [19] have extended the work of Ref. [18] to determine the parity of the Θ^+ , asserting that the sign of the spin correlation function A_{xx} agrees with the parity of the Θ^+ near threshold. Similarly, Rekaló and Tomasi-Gustafsson [25] have put forward methods for the determination of the parity of the Θ^+ by measuring the spin correlation coefficients in three different reactions, i.e., $pn \rightarrow \Lambda\Theta^+$, $pp \rightarrow \Sigma^+\Theta^+$, and $pp \rightarrow \pi^+\Lambda\Theta^+$. Thus, it seems that

the NN reactions provide a promising framework to determine the parity of the Θ^+ . The present authors have performed the calculation of the cross sections of the reaction $\vec{p}\vec{p} \rightarrow \Sigma^+\Theta^+$ near the production threshold [23], finding that the cross sections for the allowed spin configuration are estimated to be of the order of $1 \mu\text{b}$ for the positive parity Θ^+ and about one-tenth μb for the negative parity Θ^+ in the vicinity of threshold, where the S -wave component dominates.

There exist already investigations on the production of the Θ^+ in the NN interaction [27–30]. References [28,29] are concerned with the prediction of the total cross sections and Ref. [30] has explored the Θ^+ production in high-energy pp scattering. In the present work, we want to investigate the $np \rightarrow \Lambda\Theta^+$ and $np \rightarrow \Sigma^0\Theta^+$ processes with both of the positive and negative parities considered.

The present paper is organized as follows: In Sec. II, we shall compute the relevant invariant amplitudes from which the total and differential cross sections can be derived. In the subsequent section, we shall present the numerical results and discuss them. In the last section, we shall summarize and draw a conclusion.

II. EFFECTIVE LAGRANGIANS AND AMPLITUDES

The pertinent schematic diagrams for the $np \rightarrow Y^0\Theta^+$ reaction are drawn in Fig. 1. At the tree level we can consider Born diagrams of pseudoscalar K and vector K^* exchanges. The initial and final state interactions are not considered here. We will discuss briefly their effect later. As mentioned before, we treat the reactions in the case of

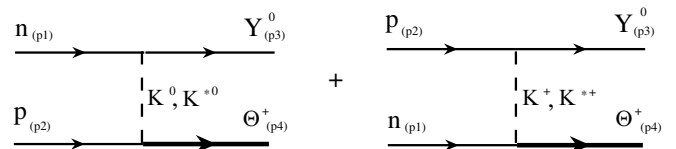


FIG. 1. Born diagrams for the $np \rightarrow Y^0\Theta^+$ reaction.

*Electronic address: sinam@rcnp.osaka-u.ac.jp

†Electronic address: hosaka@rcnp.osaka-u.ac.jp

‡Electronic address: hchkim@pusan.ac.kr

positive and negative parity Θ^+ . We distinguish the positive parity Θ^+ from the negative-parity one by expressing them as Θ^+_{\pm} and Θ^{\pm} , respectively.

We start with the following effective Lagrangians:

$$\begin{aligned}\mathcal{L}_{KNY} &= -ig_{KNY}\bar{Y}\gamma_5 K^{\dagger}N, \\ \mathcal{L}_{KN\Theta_{\pm}} &= -ig_{KN\Theta_{\pm}}\bar{\Theta}_{\pm}\Gamma_5 KN, \\ \mathcal{L}_{VNY} &= -g_{VNY}\bar{Y}\gamma_{\mu}V^{\mu}N - \frac{g_{VNY}^T}{M_Y + M_N}\bar{Y}\sigma_{\mu\nu}\partial^{\nu}V^{\mu}N, \\ \mathcal{L}_{VN\Theta} &= -g_{VN\Theta_{\pm}}\bar{\Theta}_{\pm}\gamma_{\mu}\bar{\Gamma}_5 V^{\mu}N \\ &\quad - \frac{g_{VN\Theta_{\pm}}^T}{M_{\Theta} + M_N}\bar{\Theta}_{\pm}\sigma_{\mu\nu}\bar{\Gamma}_5\partial^{\nu}V^{\mu}N,\end{aligned}\quad (1)$$

where Y , K , N , Θ , and V stand for the hyperon (Σ^0 and Λ), kaon, nucleon, Θ^+ , and vector meson fields, respectively. In order to take into account different parities for the Θ^+ in the reactions, we introduce $\Gamma_5 = \gamma_5$ for the Θ^+_{\pm} and $\Gamma_5 = \mathbf{1}_{4\times 4}$ for the Θ^{\pm} . $\bar{\Gamma}_5$ designates $\Gamma_5\gamma_5$. The isospin factor is included in Y . The $KN\Theta$ coupling constant can be determined, if we know the decay width $\Gamma_{\Theta\rightarrow KN}$.

If we choose $\Gamma_{\Theta\rightarrow KN} = 15$ MeV together with $M_{\Theta} = 1540$ MeV [1], we find that $g_{KN\Theta^+_{\pm}} = 3.78$ and $g_{KN\Theta^{\pm}} = 0.53$. If one takes a different width for $\Gamma_{\Theta\rightarrow KN}$, the coupling constant scales as a square root of the width. As for the unknown coupling constant $g_{K^*N\Theta}$, we follow Ref. [31], i.e., $g_{K^*N\Theta} = \pm|g_{KN\Theta}|/2$. The tensor coupling constant $g_{K^*N\Theta}^T$ is then fixed as follows: $g_{K^*N\Theta}^T = \pm|g_{KN\Theta}|$ as in Ref. [23]. Since the sign of the coupling constants cannot be fixed by SU(3) symmetry, we shall use both signs [31]. When their signs are the same, the $K^*N\Theta$ (magnetic) coupling strength which is the sum of the vector and tensor couplings amounts to be $1.5|g_{KN\Theta}|$. The value is similar to the one estimated in a fall apart mechanism, $g_{K^*N\Theta} = \sqrt{3}g_{KN\Theta}$ [32]. We employ the values of the KNY and K^*NY coupling constants referring to those from the new Nijmegen potential (averaged values of models NSC97a and NSC97f) [33] as well as from the Jülich-Bonn YN potential (model \tilde{A}) [34] as summarized in Table I.

The invariant Feynman amplitudes corresponding to Fig. 1 are obtained as follows:

$$\begin{aligned}i\mathcal{M} &= \left\{ i\frac{F^2(q^2)g_{KYNG_{KN\Theta_{\pm}}}}{q^2 - M_K^2}\bar{u}(p_4)\Gamma_5 u(p_2)\bar{u}(p_3)\gamma_5 u(p_1) + i\frac{F^2(q^2)g_{K^*YN}g_{K^*N\Theta_{\pm}}}{q^2 - M_{K^*}^2}\left[\bar{u}(p_4)\gamma^{\mu}\bar{\Gamma}_5 u(p_2)\bar{u}(p_3)\gamma_{\mu}u(p_1)\right. \right. \\ &\quad \left. \left. - \frac{1}{M_{K^*}^2}\bar{u}(p_4)\not{q}\bar{\Gamma}_5 u(p_2)\bar{u}(p_3)\not{q}u(p_1)\right] - i\frac{F^2(q^2)g_{K^*YN}g_{K^*N\Theta_{\pm}}^T}{2(M_N + M_Y)(q^2 - M_{K^*}^2)}\bar{u}(p_4)\gamma^{\mu}\bar{\Gamma}_5 u(p_2)\bar{u}(p_3)(\gamma_{\mu}\not{q} - \not{q}\gamma_{\mu})u(p_1) \right. \\ &\quad \left. + i\frac{F^2(q^2)g_{K^*YN}g_{K^*N\Theta_{\pm}}^T}{2(M_N + M_{\Theta})(q^2 - M_{K^*}^2)}\bar{u}(p_4)\bar{\Gamma}_5(\gamma^{\mu}\not{q} - \not{q}\gamma^{\mu})u(p_2)\bar{u}(p_3)\gamma_{\mu}u(p_1) \right. \\ &\quad \left. - i\frac{F^2(q^2)g_{K^*YN}g_{K^*N\Theta_{\pm}}^T}{4(q^2 - M_{K^*}^2)(M_N + M_Y)(M_N + M_{\Theta})}\bar{u}(p_4)(\gamma^{\mu}\not{q} - \not{q}\gamma^{\mu})\bar{\Gamma}_5 u(p_2)\bar{u}(p_3)(\gamma_{\mu}\not{q} - \not{q}\gamma_{\mu})u(p_1)\right\} \\ &\quad + [p_1 \leftrightarrow p_2],\end{aligned}\quad (2)$$

where $q = p_1 - p_3$. In order to compute the cross sections for these reactions, we need the form factors at each vertex to take into account the extended size of hadrons. For the Nijmegen potential we introduce the monopole-type form factor [35] in the form of

$$F(q^2) = \frac{\Lambda^2 - m^2}{\Lambda^2 - t}, \quad (3)$$

where m and t are the meson mass and a squared four momentum transfer, respectively. The value of the cutoff parameter is taken to be 1.0 GeV for the parameter set of the Nijmegen potential [23]. As for that of the Jülich-Bonn potential, we make use of the following form factor taken from Ref. [34]:

$$F(q^2) = \frac{\Lambda^2 - m^2}{\Lambda^2 + |\mathbf{q}|^2}, \quad (4)$$

where $|\mathbf{q}|$ is the three momentum transfer. In this case, we

take different values of the cutoff masses for each KNY vertex as follows [34]: $\Lambda_{KN\Theta} = \Lambda_{K^*N\Theta} = 1.0$ GeV, $\Lambda_{KN\Lambda} = 1.2$ GeV, $\Lambda_{K^*N\Lambda} = 2.2$ GeV, $\Lambda_{KN\Sigma} = 2.0$ GeV, and $\Lambda_{K^*N\Sigma} = 1.07$ GeV.

III. NUMERICAL RESULTS AND DISCUSSION

In this section, we present the total and differential cross sections for the reactions $np \rightarrow \Lambda^0\Theta^+$ and $np \rightarrow \Sigma^0\Theta^+$ with two different parities of Θ^+ . We first consider

TABLE I. The coupling constants used in the effective Lagrangians (1). These values are taken from Refs. [33,34] (see the text for details).

	$g_{KN\Lambda}$	$g_{K^*N\Lambda}$	$g_{K^*N\Lambda}^T$	$g_{KN\Sigma}$	$g_{K^*N\Sigma}$	$g_{K^*N\Sigma}^T$
Nijmegen	-13.26	-5.19	-13.12	3.54	-2.99	2.56
Jülich-Bonn	-18.34	-5.63	-18.34	5.38	-3.25	7.86

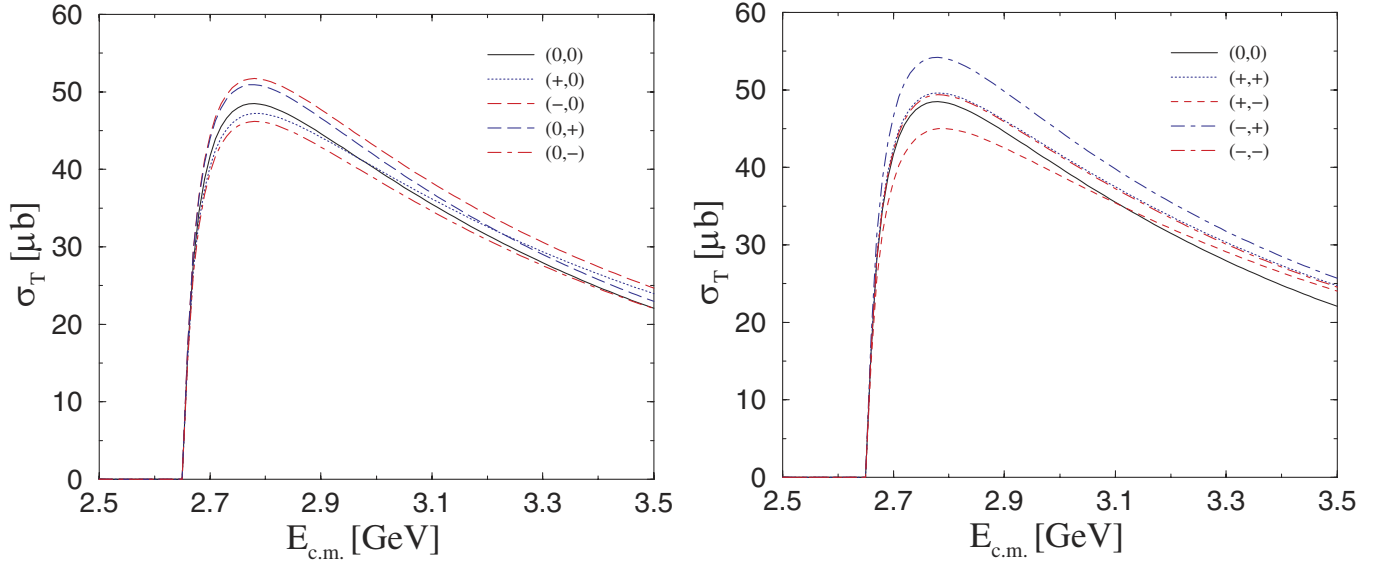


FIG. 2 (color online). The total cross sections of $np \rightarrow \Lambda \Theta_+^0$ with ten different combinations of the signs of the $K^*N\Theta$ coupling constants which are labeled by $(\text{sgn}(g_{K^*N\Theta}), \text{sgn}(g_{K^*N\Theta}^T))$. The parameter set of the Nijmegen potential with the cutoff parameter $\Lambda = 1.0$ GeV is employed.

the case of the parameter set of the Nijmegen potential. In Fig. 2, we draw the total cross sections of $np \rightarrow \Lambda \Theta_+^0$ for different signs of the coupling constants, which are labeled as $(\text{sgn}(g_{K^*N\Theta}), \text{sgn}(g_{K^*N\Theta}^T))$. We compare the results from ten different combinations of the signs. As shown in Fig. 2, the dependence on the signs is rather weak. Moreover, we find that the contribution from the K^* exchange is very tiny. The average total cross section is

obtained as $\sigma_{np \rightarrow \Lambda \Theta_+^0} \sim 40 \mu\text{b}$ in the range of the c.m. energy $E_{\text{c.m.}}^{\text{th}} \leq E_{\text{c.m.}} \leq 3.5$ GeV, where $E_{\text{c.m.}}^{\text{th}} = 2656$ MeV. Since the angular distribution for all reactions is with a similar shape, we show the results only for the case of $np \rightarrow \Lambda \Theta_+^0$ in Fig. 3.

In Fig. 4, we draw the total cross sections for the reaction $np \rightarrow \Sigma^0 \Theta_+^0$. We find that they are about 10 times smaller than those for the reaction $np \rightarrow \Lambda \Theta_+^0$.

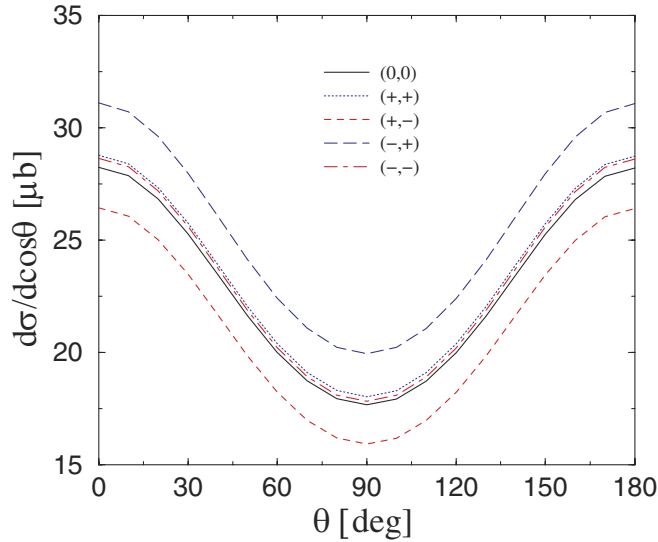


FIG. 3 (color online). The differential cross sections for the reaction $np \rightarrow \Lambda \Theta_+^0$ at $E_{\text{c.m.}} = 2.7$ GeV with five different combinations of the signs of the $K^*N\Theta$ coupling constants as labeled by $(\text{sgn}(g_{K^*N\Theta}), \text{sgn}(g_{K^*N\Theta}^T))$. The parameter set of the Nijmegen potential with the cutoff parameter $\Lambda = 1.0$ GeV is employed.

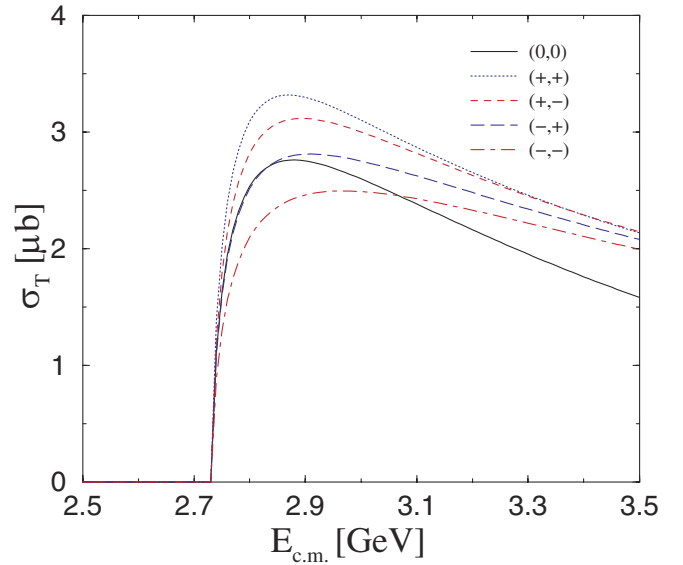


FIG. 4 (color online). The total cross sections for the reaction $np \rightarrow \Sigma^0 \Theta_+^0$. The parameter set of the Nijmegen potential with the cutoff parameter $\Lambda = 1.0$ GeV is employed. The notations are the same as in Fig. 3.

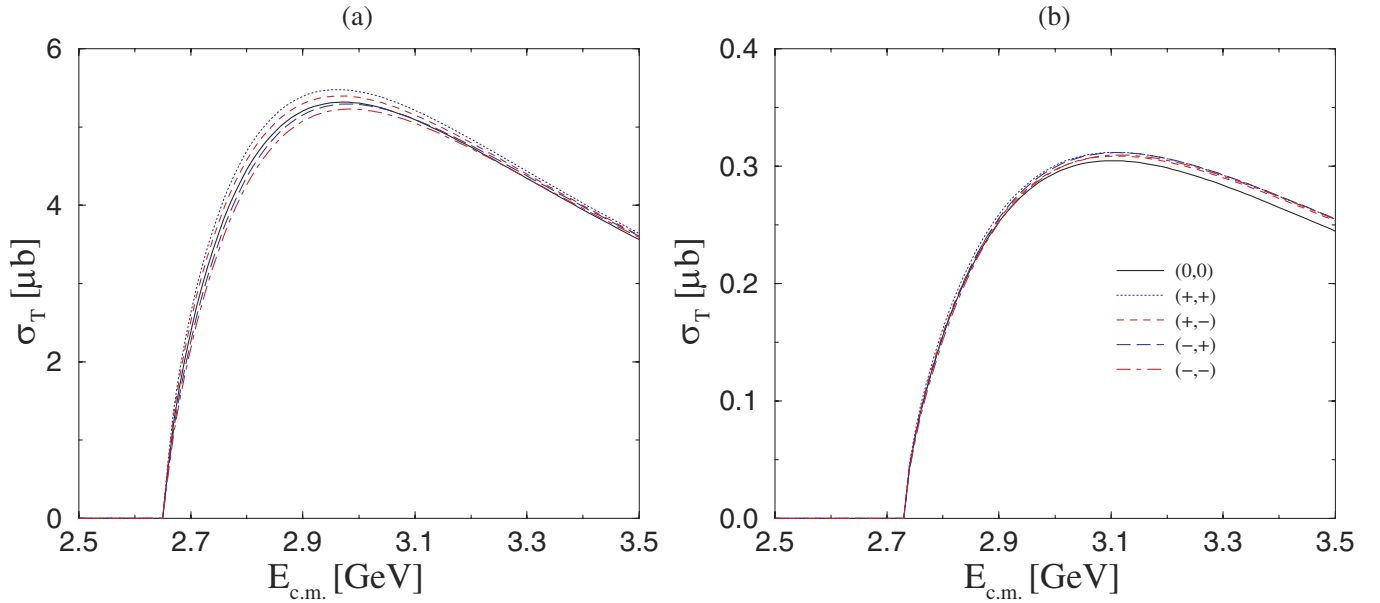


FIG. 5 (color online). The total cross sections of $np \rightarrow \Lambda \Theta^\pm$ in the left panel (a) and $np \rightarrow \Sigma^0 \Theta^\pm$ in the right panel (b). The parameter set of the Nijmegen potential with the cutoff parameter $\Lambda = 1.0$ GeV is employed. The notations are the same as in Fig. 3.

The corresponding average total cross section is found to be $\sigma_{np \rightarrow \Sigma^0 \Theta^\pm} \sim 2.0 \mu\text{b}$ in the range of the c.m. energy $E_{\text{c.m.}}^{\text{th.}} \leq E_{\text{c.m.}} \leq 3.5$ GeV, where $E_{\text{c.m.}}^{\text{th.}} = 2733$ MeV. It can be easily understood from the fact that the ratio of the coupling constants $|g_{KN\Lambda}/g_{KN\Sigma}| = 3.74$ is rather large and the contribution from K exchange is dominant.

As for the negative parity Θ^+ , we show the results in Fig. 5. Once again we find that the contribution of the K^* exchange plays only a minor role. We observe on average

that $\sigma_{np \rightarrow \Lambda \Theta^\pm} \sim 5.0 \mu\text{b}$ and $\sigma_{np \rightarrow \Sigma^0 \Theta^\pm} \sim 0.3 \mu\text{b}$ in the range of the c.m. energy $E_{\text{c.m.}}^{\text{th.}} \leq E_{\text{c.m.}} \leq 3.5$ GeV. They are almost 10 times smaller than those of Θ_\pm^+ . This behavior can be interpreted dynamically by the fact that a large momentum transfer ~ 800 MeV enhances the P -wave coupling of the Θ_\pm^+ more than the S -wave one of the Θ_\pm^+ .

In Fig. 6, we show the total cross sections of the reactions for the Θ_\pm^+ with the parameter set of the

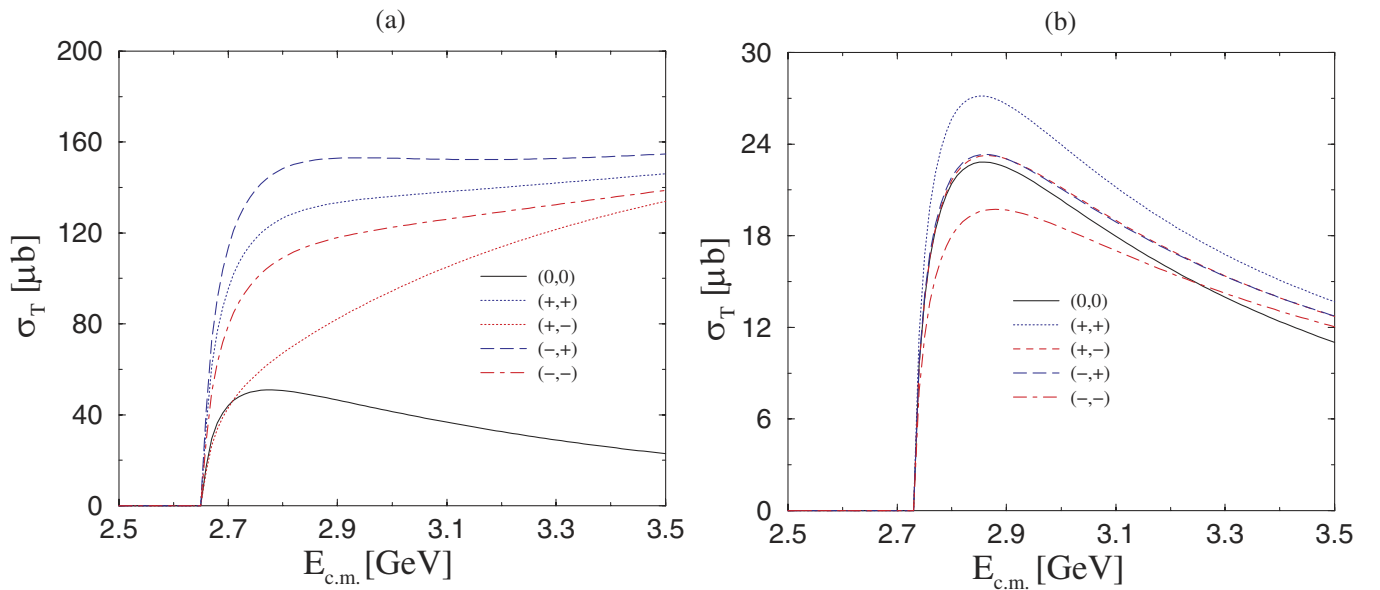


FIG. 6 (color online). The total cross sections of $np \rightarrow \Lambda \Theta_\pm^+$ in the left panel (a) and $np \rightarrow \Sigma^0 \Theta_\pm^+$ in the right panel (b). The parameter set of the Jülich-Bonn potential is employed. The notations are the same as in Fig. 3.

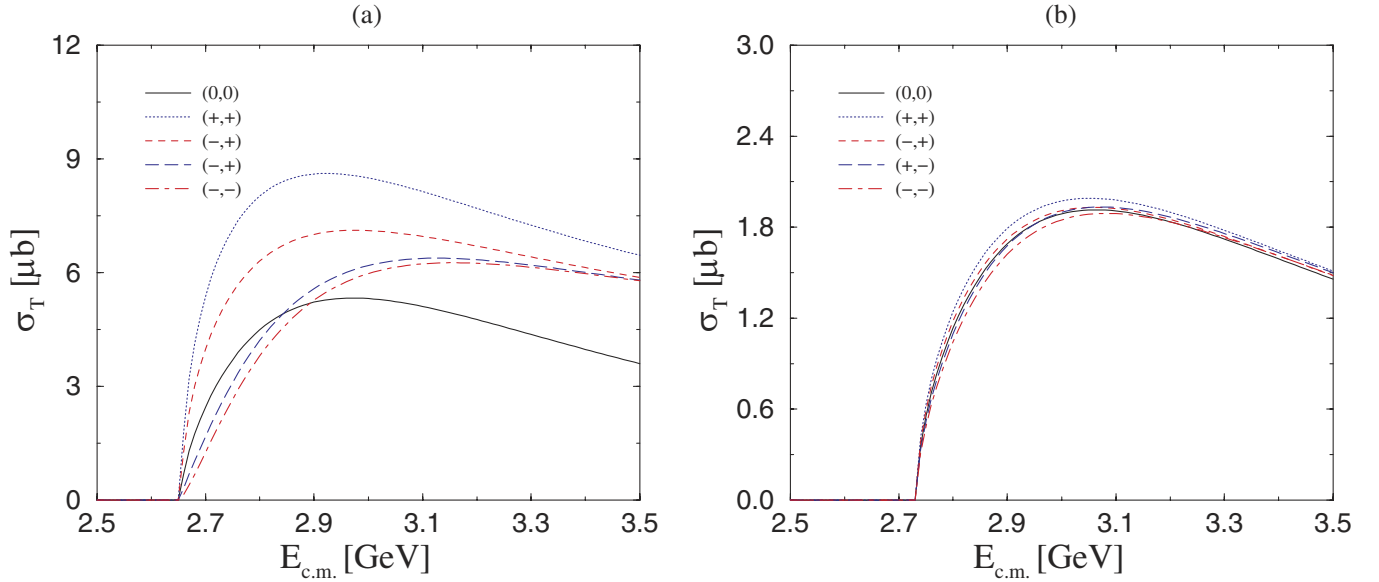


FIG. 7 (color online). The total cross sections of $np \rightarrow \Lambda \Theta^\pm$ in the left panel (a) and $np \rightarrow \Sigma^0 \Theta^\pm$ in the right panel (b). The parameter set of the Jülich-Bonn potential is employed. The notations are the same as in Fig. 3.

Jülich-Bonn potential. Here, different cutoff parameters are employed at different vertices as mentioned previously. We find that the contribution from the K^* exchange turns out to be larger in the $np \rightarrow \Lambda \Theta^\pm$ reaction than in the $np \rightarrow \Sigma^0 \Theta^\pm$. This can be easily understood from the fact that the Jülich-Bonn cutoff parameter $\Lambda_{K^*N\Lambda}$ is chosen to be approximately twice as large as that of the $KN\Lambda$ vertex, while the value of the $\Lambda_{K^*N\Sigma}$ is about 2 times smaller than that of the $\Lambda_{KN\Sigma}$. The average total cross sections are obtained as follows: $\sigma_{np \rightarrow \Lambda \Theta^\pm} \sim 100 \mu\text{b}$ and $\sigma_{np \rightarrow \Sigma^0 \Theta^\pm} \sim 20 \mu\text{b}$ in the range of the c.m. energy $E_{\text{c.m.}}^{\text{th.}} \leq E_{\text{c.m.}} \leq 3.5 \text{ GeV}$.

In Fig. 7, the total cross sections for Θ^\pm are drawn. In this case, the average total cross sections are given as follows: $\sigma_{np \rightarrow \Lambda \Theta^\pm} \sim 6.0 \mu\text{b}$ and $\sigma_{np \rightarrow \Sigma^0 \Theta^\pm} \sim 2.0 \mu\text{b}$ in the same range of the c.m. energy. The results for the negative parity Θ^\pm are about 15 times smaller than those of Θ^\pm .

Compared to the results with the parameter set of the Nijmegen potential, those with the Jülich-Bonn one are rather sensitive to the signs of the coupling constants. It is due to the fact that the cutoff parameters taken from the Jülich-Bonn potential are different at each vertex. If we had taken similar values of the cutoff parameters for the Nijmegen potential, we would have obtained comparable results to the case of the Jülich-Bonn potential.

IV. SUMMARY AND CONCLUSION

Motivated by a series of recent works [17–25], we have studied the reactions $np \rightarrow \Lambda \Theta^+$ and $np \rightarrow \Sigma^0 \Theta^+$, employing both of the negative and positive parities for the

Θ^+ . We have considered K and K^* meson exchanges in the Born approximation. We have chosen for the mass of the Θ^+ and coupling constant of the $KN\Theta$ vertex typical values which are not inconsistent with the original observation [1]. Then the strength of the K^* coupling to the Θ^+ has been estimated by using SU(3) symmetry [31]. It turned out that the contribution of K exchange was dominant. The dependence on the K^* exchange is not very significant within the theoretically expected range for the $K^*N\Theta$ coupling constant [32]. The difference between the results of Nijmegen and Jülich-Bonn potentials arises dominantly from the different coupling constants and cutoff parameters for the KNY vertices. The Jülich-Bonn potential adopts larger coupling constants and cutoff parameters which yields significantly larger cross sections than the Nijmegen potential.

We have found that $\sigma_{np \rightarrow Y^0 \Theta^\pm} \gg \sigma_{np \rightarrow Y^0 \Theta^\pm}$, as shown in Table II where we have summarized the total cross sections averaged in the energy region $E_{\text{c.m.}}^{\text{th.}} < E_{\text{c.m.}} < 3.5 \text{ GeV}$, where $E_{\text{c.m.}}^{\text{th.}} = 2656 \text{ MeV}$ for the Λ production and 2733 MeV for Σ production. Concerning the absolute values, it should be pointed out that they must change if a different value of $\Gamma_{\Theta \rightarrow KN}$ is used as proportional to it.

TABLE II. The total cross sections averaged in the energy region $E_{\text{c.m.}}^{\text{th.}} < E_{\text{c.m.}} < 3.5$.

Final hyperon	Nijmegen		Jülich-Bonn	
	Λ	Σ^0	Λ	Σ^0
$\sigma_{P=+1} (\mu\text{b})$	40	2.0	100	20
$\sigma_{P=-1} (\mu\text{b})$	5.0	0.3	6.0	2.0

Here we have used $\Gamma_{\Theta \rightarrow KN} = 15$ MeV. Recent experiment and analysis indicate narrower widths [36,37]. For instance, if we take $\Gamma_{\Theta \rightarrow KN} \sim 5$ MeV, then the cross sections are reduced by a factor 3. Furthermore, the initial state interaction also changes the present estimate significantly. Typically it can reduce the total cross sections by about a factor 3 as discussed in hyperon productions [38].

As suggested by Refs. [18–21,23–25], the NN induced reactions will provide a good framework to determine the parity of the Θ^+ , though it might still require an experimental challenge. However, we anticipate that we would provide a guideline together with recent works for future experiments to pin down the parity of the Θ^+ .

ACKNOWLEDGMENTS

H. Ch. K. is grateful to J. K. Ahn, C. H. Lee, and I. K. Yoo for valuable discussions and comments. The work of H. Ch. K. is supported by the KOSEF Grant No. R01-2001-00014 (2003). He also acknowledges the support from the 21st COE Program “Towards A New Basic Science: Depth and Synthesis” (Osaka University), which made it possible for him to visit the RCNP, where a part of this work was carried out. The work of S. I. N. has been supported by the Ministry of Education, Science, Sports and Culture of Japan. A. H. is supported in part by the Grant for Scientific Research [(C) No. 16540252] from the Ministry of Education, Culture, Science and Technology, Japan.

-
- [1] LEPS Collaboration, T. Nakano *et al.*, Phys. Rev. Lett. **91**, 012002 (2003).
 - [2] D. Diakonov, V. Petrov, and M.V. Polyakov, Z. Phys. A **359**, 305 (1997).
 - [3] DIANA Collaboration, V.V. Barmin *et al.*, Yad. Fiz. **66**, 1763 (2003) [Phys. At. Nucl. **66**, 1715 (2003)].
 - [4] CLAS Collaboration, S. Stepanyan *et al.*, Phys. Rev. Lett. **91**, 252001 (2003); CLAS Collaboration, V. Kubarovsky and S. Stepanyan, AIP Conf. Proc. **698**, 543 (2004).
 - [5] SAPHIR Collaboration, J. Barth, hep-ex/0307083.
 - [6] HERMES Collaboration, A. Airapetian *et al.*, Phys. Lett. B **585**, 213 (2004).
 - [7] SVD Collaboration, A. Aleev *et al.*, hep-ex/0401024.
 - [8] A. E. Asratyan, A. G. Dolgolenko, and M. A. Kubantsev, Yad. Fiz. **67**, 704 (2004) [Phys. At. Nucl. **67**, 682 (2004)].
 - [9] NA49 Collaboration, C. Alt *et al.*, Phys. Rev. Lett. **92**, 042003 (2004).
 - [10] R. L. Jaffe and F. Wilczek, Phys. Rev. Lett. **91**, 232003 (2003); M. Karliner and H. Lipkin, hep-ph/0307243; S. Capstick, Ph. R. Page, and W. Roberts, Phys. Lett. B **570**, 185 (2003); C. E. Carlson, Ch. D. Caronne, H. J. Kwee, and V. Nazaryan, Phys. Lett. B **573**, 101 (2003); E. Shuryak and I. Zahed, Phys. Lett. B **589**, 21 (2004).
 - [11] M. Praszalowicz, in *Proceedings of the Workshop on Skyrmions and Anomalies*, edited by M. Jeżabek and M. Praszalowicz (World Scientific, Singapore, 1987), p. 112; Phys. Lett. B **575**, 234 (2003); H. Weigel, Eur. Phys. J. A **2**, 391 (1998); H. Wälliser and V. B. Kopeliovich, Nucl. Phys. **B660**, 156 (2003); A. Hosaka, Phys. Lett. B **571**, 55 (2003); D. Diakonov and V. Petrov, Phys. Rev. D **69**, 056002 (2004); H. C. Kim and M. Praszalowicz, Phys. Lett. B **585**, 99 (2004).
 - [12] N. Itzhaki, I. R. Klebanov, P. Ouyang, and L. Rastelli, Nucl. Phys. **B684**, 264 (2004).
 - [13] D. E. Kahana and S. H. Kahana, Phys. Rev. D **69**, 117502 (2004); F. Huang, Z. Y. Zhang, Y. W. Yu, and B. S. Zou, Phys. Lett. B **586**, 69 (2004).
 - [14] S. L. Zhu, Phys. Rev. Lett. **91**, 232002 (2003); J. Sugiyama, T. Doi, and M. Oka, Phys. Lett. B **581**, 167 (2004).
 - [15] F. Csikor, Z. Fodor, S. D. Katz, and T. G. Kovacs, J. High Energy Phys. **11** (2003) 070; S. Sasaki, Phys. Rev. Lett. **93**, 152001 (2004).
 - [16] Y. Oh, H. Kim, and S. H. Lee, Phys. Rev. D **69**, 014009 (2004); T. Hyodo, A. Hosaka, and E. Oset, Phys. Lett. B **579**, 290 (2004); S. I. Nam, A. Hosaka, and H.-Ch. Kim, Phys. Lett. B **579**, 43 (2004).
 - [17] K. Nakayama and K. Tsushima, Phys. Lett. B **583**, 269 (2004).
 - [18] A. W. Thomas, K. Hicks, and A. Hosaka, Prog. Theor. Phys. **111**, 291 (2004).
 - [19] C. Hanhart *et al.*, Phys. Lett. B **590**, 39 (2004).
 - [20] Q. Zhao and J. S. Al-Khalili, Phys. Lett. B **585**, 91 (2004).
 - [21] B. G. Yu, T. K. Choi, and C. R. Ji, Phys. Rev. C **70**, 045205 (2004).
 - [22] C. E. Carlson, C. D. Carone, H. J. Kwee, and V. Nazaryan, Phys. Rev. D **70**, 037501 (2004).
 - [23] S. I. Nam, A. Hosaka, and H. C. Kim, Phys. Lett. B **602**, 180 (2004).
 - [24] T. Mehen and C. Schat, Phys. Lett. B **588**, 67 (2004).
 - [25] M. P. Rekaló and E. Tomasi-Gustafsson, Phys. Lett. B **591**, 225 (2004).
 - [26] T. Nakano (private communication).
 - [27] M. V. Polyakov, A. Sibirtsev, K. Tsushima, W. Cassing, and K. Goetze, Eur. Phys. J. A **9**, 115 (2000).
 - [28] W. Liu and C. M. Ko, Phys. Rev. C **68**, 045203 (2003).
 - [29] Y. Oh, H. Kim, and S. H. Lee, Phys. Rev. D **69**, 074016 (2004).
 - [30] M. Bleicher, F. M. Liu, J. Aichelin, T. Pierog, and K. Werner, Phys. Lett. B **595**, 288 (2004).
 - [31] W. Liu, C. M. Ko, and V. Kubarovsky, Phys. Rev. C **69**, 025202 (2004).
 - [32] F. E. Close and J. J. Dudek, Phys. Lett. B **586**, 75 (2004).
 - [33] V. G. J. Stokes and Th. A. Rijken, Phys. Rev. C **59**, 3009 (1999).

- [34] A. Reuber, K. Holinde, and J. Speth, Nucl. Phys. **A570**, 543 (1994).
- [35] R. Machleidt, K. Holinde, and C. Elster, Phys. Rep. **149**, 1 (1987).
- [36] ZEUS Collaboration, S. Chekanov *et al.*, Phys. Lett. B **591**, 7 (2004).
- [37] A. Sibirtsev, J. Haidenbauer, S. Krewald, and U.G. Meissner, Phys. Lett. B **599**, 230 (2004).
- [38] C. Hanhart, Phys. Rep. **397**, 155 (2004).